Simulation of Grain-Straw Separation by Discrete Element Modeling with Bendable Straw Particles

Bart Lenaerts[a,*], Thomas Aertsen[a], Engelbert Tijskens[a], Bart De Ketelaere[a], Herman Ramon[a], Wouter Saeys[a]

[a] *BIOSYST-MeBioS, Faculty of Bioscience Engineering, KU Leuven, Kasteelpark Arenberg 30, B-3001 Leuven, Belgium*

Abstract

The combine harvester owes its name to the integration of the whole chain of grain harvesting steps in one machine. Running these interdependent processes simultaneously requires insight in the influence of crop factors and adjustments on the individual processes and the consequences for downstream processes. This paper introduces changes to the Discrete Element Method (DEM) in order to be suitable for the simulation of grain-straw separation, which is one of the most critical processes in the combine harvester. Segmented bendable straw particles have been constructed in the DEMeter++ simulation environment and their physical properties have been calibrated with realistic straw properties. The use of these particles for modeling separation has been validated by reconstructing an existing separation experiment by Beck (1992) in DEMeter++ and comparing the simulation result with the experiment. Once validated, the practical use of the simulation framework to assess the sensitivity of separation to crop properties is illustrated.

Keywords:

DEM, Bendable cylindrical particles, Separation, Straw, Grain, Combine harvester

Preprint submitted to Computers and Electronics in Agriculture *October 29, 2013*

* Corresponding author
Tel.: +32 16 377087; Fax.: +32 16 328590
E-mail address: bart.lenaerts@biw.kuleuven.be

1. Introduction

Grain and straw have a different shape and density. Grain can therefore be separated from straw by accelerating the mixture. In the separation section of a combine harvester, the grain kernels which have been released from the ears through threshing have to be expelled from the straw layer. The necessary acceleration is induced by the action of oscillating walkers or centrifugation. Obviously, as the combine harvester is a continuous-flow machine, the residence time of the grain-straw mixture in the threshing and separation unit limits the time available for the grain to migrate through the straw layer to the walker's surface. Grain kernels that are threshed but are still lodged in the straw layer when it leaves the machine are called separation losses. Modern combine harvesters separate more than 100 tons of this grain and straw mixture per hour, meanwhile, the acceptable grain loss over all sub-processes is typically not higher than 1%. The separation and cleaning losses usually have the biggest share. Designing a new separation section and optimizing its settings is not straightforward due to the complex interaction between the machine and the crop. In addition, for an optimal operation of existing separation sections, quantitative insight in the interference of crop, design and settings is required. An accurate model describing the separation process in a grain harvester would allow to (Kutzbach, 2003):

- Reduce the test expenditure
- Improve the understanding of the fundamental relationships
- Make a targeted choice on future improvements

- Simulate the influences of different parameters
- Estimate possible performance increases

A modeling framework for separation should be able to describe the particle interactions adequately and to include particle properties involved. The models which have been reported in literature (summarized e.g. in Kutzbach (2003)) fit well to the experimental data, but their empirical nature typically limits their practical relevance to specific crop and machine characteristics. Furthermore, the effect of crop properties on separation is mostly unclear as different crop property combinations can give the same end result in separation. However, the importance of their influence on the separation process has been underlined by Hall and Husman (1981), Shandilya (1987) and Srivastava et al. (1990). As many of these properties are interdependent (Hall and Husman, 1981; Huisman, 1978) it is impossible to correlate individual crop properties to separation performance statistically. Moreover, the biological variability of the crop in the field is high and the strong effect of feedrate on separation will shade the effect of other factors. In order to have better control over the variables involved and to be able to monitor the process more accurately, laboratory experiments on separation have been carried out under known conditions of crop weight and properties. In this context an idealized experiment representative of separation on straw walkers, employed by Baader et al. (1969) has been repeated in several research works in the last decades, for instance by Huisman (1978) and Beck (1992). The setup consists of a straw layer contained in a vertically, sinusoidally oscillating box. After the straw has been agitated for a certain time, a layer of grain kernels is released at once on top of the oscillating straw layer. Grain passage through

the grating at the bottom of the box is recorded in function of time. The grain sinks through the straw layer, while it disperses laterally. This results in a sigmoidal curve of the separated fraction in function of time. The lower the area density of the straw layer, the faster the kernels can sink and the steeper the separation curve will be. Shandilya (1987) used a similar setup but with horizontal instead of vertical shaking.

So far little is known about the mechanical interactions between grain and straw particles during separation. This would yield fundamental insight into the influence of the properties of the particles involved on the performance. As this interaction takes place at the particle level, a modeling framework on this level should be set up. When modeling the behaviour of a collection of particles, like grain kernels, Discrete Element Modeling (DEM) is a logical choice as it allows to model the behaviour of each kernel through its interactions with the other kernels and the system elements. Also in agricultural processes, DEM is more and more used for simulating particulate processes as e.g. grain flow in silos (González-Montellano et al., 2011), fertilizer spreading (Tijskens et al., 2003; Van Liedekerke et al., 2009) or manure handling and land application equipment (Landry et al., 2006). In this way, the influence of particle properties and boundary conditions can be assessed with a set of in silico experiments that can be run in parallel. However, simulating the straw particles with discrete elements is more challenging as straw has a large aspect ratio, resulting in a clear orientation. To study the alignment of straw particles and cutting blades in the chopper section of a combine, Kattenstroth et al. (2011) employed a Discrete Element Model with straw particles constructed with connected spheres. However, straw is bendable, a

property which is expected to have an important impact on the separation process. To the authors' knowledge, DEM simulation with bendable straw particles has not been reported in scientific literature to date.

Therefore, in this study a discrete element approach including bendable straw has been implemented in the DEMeter++ (Tijskens et al., 2003) software. Once the straw particles have been constructed, the crop properties can be easily defined and changed independently. This makes it relatively easy to study the sensitivity of the separation profile with reference to the individual crop properties. The Discrete Element Model with bendable straw particles is then used to simulate the stationary separation experiment described by Beck (1992). As the properties of the straw and grain kernels employed in the real-life experiment are not known, an experimental design of crop properties is set up and a simulation is run with each set of crop properties. The validation then consists of a statistical comparison of simulated separation profiles to the reported experimental profiles. Once validated, the different separation profiles can be used to perform a sensitivity analysis of the crop properties on the separation rate.

2. Discrete Element Modeling framework

The Discrete Element Method (DEM), also called Discrete Element Modeling, is a numerical technique to model the motion of an assembly of particles which interact with each other through collisions. It was originally developed by Cundall and Strack (1979) for predicting the behaviour of soil grains and belongs to the group of "Particle Based Simulations". By applying DEM, the trajectory of each particle in a system can be obtained using a numerical

time integration scheme. At each time step, all forces acting on the particles like contact forces, body forces, etc. are summed. Newton's equations of motion are then integrated to obtain the velocity and position of each particle at the next time step (Tijskens et al., 2003). A DEM problem can be described mathematically as a system of non-linear differential ODE's formed by Newton's equations of translation (Eq. 1) and rotation (Eq. 2) for each individual particle i:

$$m_i \mathbf{a}_i = \mathbf{G}_i + \sum_c \mathbf{F}_{ci}, \tag{1}$$

$$\mathbf{I}_i \boldsymbol{\alpha}_i = \mathbf{H}_i + \sum_c \mathbf{r}_{ci} \times \mathbf{F}_{ci}, i = 1, ..., N. \tag{2}$$

$\mathbf{a}_i$ and $\boldsymbol{\alpha}_i$ are the translational and rotational acceleration of the ith particle and $\mathbf{m_i}$ and $\mathbf{I}_i$ are the mass and inertia tensor. $\mathbf{G}_i$ and $\mathbf{H}_i$ are the body force and moment that act on the ith particle. Additionally $\mathbf{F}_{ci}$ is the contact force acting on the particle caused by the cth contact with a neighboring particle. Finally, $\mathbf{r}_{ci}$ represents the position vector of that c-th contact with respect to the center of mass of the particle i

The DEM algorithm of the grain-straw separation has following structure:

System initialization. The state of the system is completely determined at t=0. The initial dimensions of all particles and their initial positions and velocities are defined. Also the time discretization step (Δt) is chosen.

At each time step:

- *Contact detection.* All current contacts between particles should be de-

tected. To find all these contacts in a computationally efficient way, the grid based contact detection algorithm proposed by Iwai et al. (1999) is used.

- *Contact forces.* For each actual contact between particle i and another particle j the contact force F_{ij} is calculated. Particles in DEM are considered as rigid bodies with point contacts. Deformation during impact is simulated by allowing particles to overlap slightly. Consequently the contact force between two particles is related to this virtual overlap. The applied contact model can be divided into two parts: a normal and a tangential part. A linear viscoelastic model, namely a linear spring-damper, is used as normal contact force model (Tijskens et al., 2003), whereas the Werner-Haff model (Haff and Werner, 1986) is used as tangential contact force model (Haff and Werner, 1986).

- *Compilation of forces and moments.* The vectors of the forces working on each individual particle i are summed and also used to calculate moments. These resulting forces and moments are then employed in Newton's equations of motion (Eq.1 and 2).

- *Integration of the equations of motion.* Newton's equations of motion are integrated numerically to obtain the new positions and velocities of each individual particle i at time $t + \Delta t$. Numerical integration schemes are mostly kept very basic in DEM as the numerical errors of these schemes are much less important than the approximate nature of the contact force models. As for this reason the second order accurate Leap-frog time integration algorithm is used (Tijskens et al., 2003).

After the appropriate settings of the DEMeter++ program have been chosen, the particles are constructed. This is described in the next subsection.

2.1. Grain particles in DEMeter++

Grain kernels are approximated by spheres. This is a rough approximation of real grain kernels, rather having an ellipsoid shape. More realistic grain kernels could be created by using composite particles made up of several overlapping spheres. However, the additional computational cost of composite particles would have made it infeasible to simulate the experiment within a reasonable time. As characterizing the grain shape with only one dimension led to a successful approximation of the separation curve in Gregory and Fedler (1986) and Shandilya (1987) it is expected that this assumption can be safely made if the right dimension of the grain is chosen as diameter of the spheres.

2.2. Straw particles in DEMeter++

A realistic straw stalk should be flexible in all directions, be extensible and compressible in the axial and radial direction and have frictional characteristics. To satisfy all these requirements segmented straw particles have been developed in DEMeter++. Each segment consists of a rigid hollow cylinder connected to its adjacent cylinders by spherical joints. At both ends of the straw particle an additional joint is placed, as can be seen in Fig. 1. The joints are responsible for the flexibility of the particle. At each intersection between a cylinder and a joint a virtual disk is present, so every joint consists of two disks. These two disks are interconnected with six linear spring-dampers, positioned in an axisymmetric pattern. The stiffness of the

springs determines the bending resistance of the joint and the dampers prevent the joint from oscillating by dissipating the received energy. The springs are not loaded if the two disks coincide. The tensile stiffness of each segment of the straw particle is provided by one extra set of a spring and damper. They are attached to the two disks belonging to that particular segment.

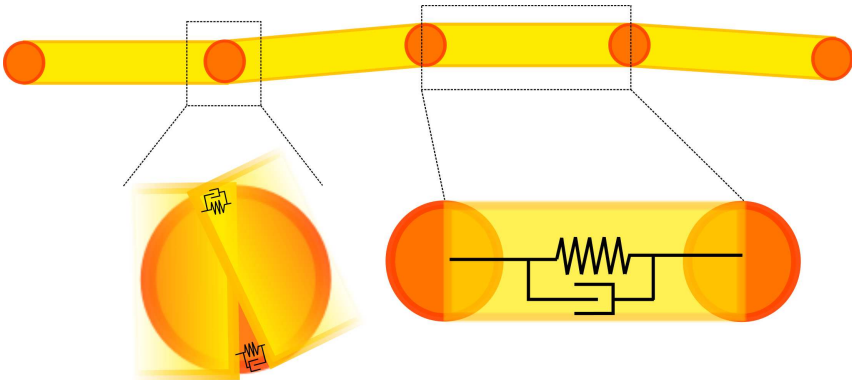

Figure 1: Bendable straw in DEM

2.3. Calibration of particle properties

As the grain particles are conceived as spherical particles, their properties can be directly set in DEMeter++. The proposed construction for bendable straw on the other hand needs calibration by adjustment of the different spring and damper constants in order to obtain a realistic behaviour. As most of the mechanical properties of straw have been described in literature these can be used here. The ones that are considered relevant for separation are summarized together with their source in Table 1. As the mechanical properties of straw can vary considerably, parameter ranges are given instead of single values. As no values for the radial compressibility of the straw stalks

were found in literature, this property was determined experimentally as will be described in section 2.3.3.

Table 1: Properties of wheat straw employed in the simulations

Straw properties	minimum	maximum	source
length (m)	0.7		b
radius (m)	0.00142	0.001725	c, d, i
wall thickness (m)	0.000527	0.000957	c, d
density (kg/m^3)	195.97	226,62	c, d
E_b(GPa)	1.283	5.995	c, d, g
friction (straw-straw)[1]	0.3		h
friction (straw-steel)[2]	0.3		h
tension modulus (GPa)	4.16	8.22	f
Grain properties	minimum	maximum	source
minor axis diameter (m)	0.00254	0.0035	a, e
kernel weight (kg)	0.00003366	0.00005084	a

Sources: a:Mohsenin et al. (1986); b:Beck (1992); c:O'Dogherty et al. (1995); d:Annoussamy et al. (2000); e:Stroshine (2000); f:Wright et al. (2005); g:Tavakoli et al. (2008); h:Sitkei (1986); i:own measurements.

[1] Moisture content 25% W.B.; [2] Moisture content unavailable

2.3.1. Straw bending stiffness

The segmented straw stalks in DEM are calibrated to obtain a realistic bending behaviour. Most researchers (e.g. Annoussamy et al. (2000) for wheat straw) measured the bending stiffness of wheat straw using a three-

point bending test. Straw stalks are cut into their different internodes and each internode is placed on two rounded supports positioned a distance L apart and loaded in the middle by a moving support. By measuring the applied force (F_b), the outer radius of the stalk (R) and the thickness of the stem wall (e), the Young's modulus in bending(E_b) was calculated for each internode using formulas (3) and (4) with I_b the second moment of area of a tubular cross-section.

$$I_b = \frac{\pi[R^4 - (R-e)^4]}{4} \tag{3}$$

$$E_b = \frac{\frac{L^3(dF_b/dl)}{48}}{I_b} \tag{4}$$

The Young's moduli obtained from Annoussamy et al. (2000) can now be used to determine the bending stiffness (dF_b/dl) of a straw stalk with the same length as the straw stalks employed by Beck (1992) (0.7 m) by performing the reverse calculation. The distance between the supports is then chosen to be 0.667 m, which establishes a 2.5% margin at each side so that the particle is not pushed off the supports during bending. Annoussamy et al. (2000) reported a bending stiffness value for each internode. To obtain a general Young's modulus in bending for the whole straw particle a weighted average is taken with the internode lengths as weights. The result of this averaging can be found in Table 1. Next, Eqs. 3 and 4 are used to derive the bending stiffness dF_b/dl. To apply the obtained value for the bending stiffness dF_b/dl to the virtual straw a link has to be established between the linear spring-dampers in between the different segments and the calculated bending stiffness. This is done by successive simulations of the three-point bending test in DEMeter++ (Fig. 2) until the slope of the simulated curve

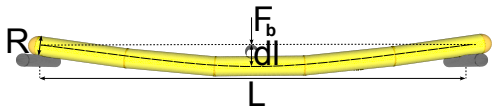

Figure 2: Simulated three-point bending test

coincides with the experimental one. By comparing the slope of the simulated force-displacement curve with the desired dF_b/dl, the stiffness of the springs and the damping factor of the dampers can be adjusted until the straw shows the right behaviour.

2.3.2. Straw elongation stiffness

A second characteristic of the straw stalks that can be controlled in the DEM simulations, is their elongation stiffness. As illustrated in Fig. 1, each segment contains a linear spring-damper mounted in between the disks at each end. This system of parallel springs and dampers is not loaded at the initial straw length. Wright et al. (2005) determined the tension moduli for two varieties of wheat, summarized in Table 1, the smallest value corresponds to the *Westbred 936* variety, the largest one to the *Amidon* variety. As Young's modulus is defined as the ratio of stress and strain (Eq.5) and using the definition of the spring constant $k = F_e/\Delta L$, a general spring constant can be calculated easily by combining both equations. As before, the length L of the straw stalk is set to 0.7 m.

$$E_e = \frac{F_e/A}{\Delta L/L} \tag{5}$$

$$k = \frac{E_e \cdot A}{L} \tag{6}$$

Each segment contains a spring, so the tension modulus of an aggregate straw particle is the result of a series of springs. The spring constant for

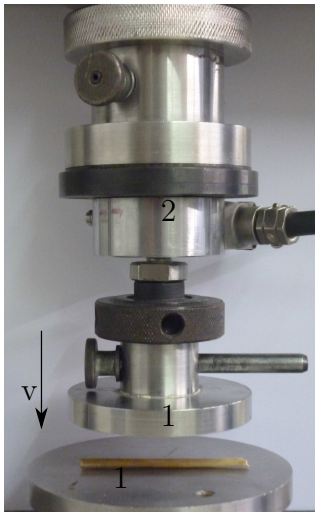

Figure 3: Experimental setup consisting of two approaching flat plates (1) and a load cell (2)

each individual spring should then be the overall spring constant multiplied with the number of segments n.

2.3.3. Straw radial compressibility

The radial compressibility of a straw stalk specifies how the contact between individual straw stalks will occur. The stiffer the material, the larger the impact. In the DEM simulations, this compressibility is contained in the normal contact force model (section 2) as a linear spring-damper. As little is found in literature on single straw compression, a compression experiment was conducted using a Universal Testing System (Type 005.00, *UTS Testsysteme*, Ulm, Germany). The experimental setup is depicted in Fig. 3. A 0.06 m long straw stalk was compressed between two flat plates. The compression force is measured by a load cell (*U1, Hottiger Baldwin Messtechnik*, Darmstadt, Germany) with a range of 200 N. The measurement is repeated

for five straw stalks with 3 internodes each. The resulting force-displacement curve is shown in (Fig. 4). Although the compression process is definitely

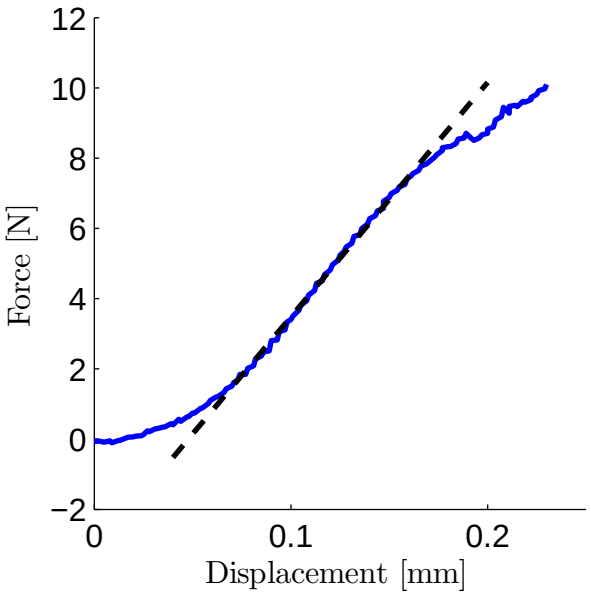

Figure 4: Force-displacement curve

non-linear, which can be seen in Fig. 4, it will be approached in a linear way. Only the first, linear elastic part of the force-displacement curve is taken into account, the deflection in the last part is due to cracking of the particles which is unlikely to happen in the separation experiment, given the low straw area densities employed in the experiments and the relatively high force at which cracking occurs. A straight line is fitted on these measurement points by a least-squares regression. The slope of this trend line is a measure of the compression stiffness. The average of all 15 measured internodes is taken to obtain a realistic value for the compression stiffness of an individual straw stalk of 0.06m. As illustrated in Fig. 5 the stalk forms a system of

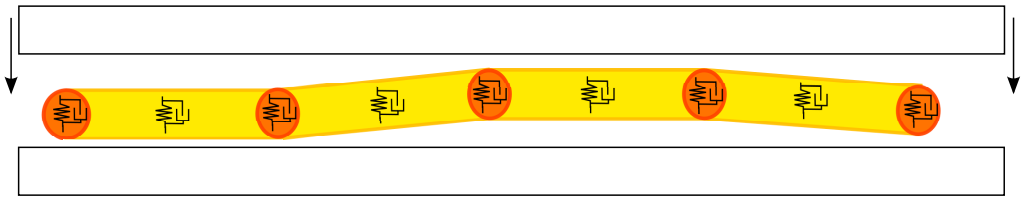

Figure 5: DEM equivalent of the UTS compression test

multiple springs and dampers in parallel in the radial direction so that the compression stiffness obtained from the UTS measurement has to be divided by the sum of the number of spheres and cylinders that constitute a straw particle to obtain the individual spring constants.

2.3.4. Straw friction

The Werner and Haff model is used to model the tangential contact (friction). This model requires a friction coefficient. Sitkei (1986) reported a friction coefficient of straw on galvanized steel of 0.3 and a coefficient for friction between straw particles in function of their moisture coefficient and mutual angle. It is, however, computationally not efficient to include an angle-dependent friction coefficient in the simulations. As simulations with the upper and lower limits of the straw-straw friction values reported by Sitkei (1986) did not result in significant differences, the average value of 0.3 for dry straw was used. Moreover Sitkei (1986) reported that at low moisture contents like the one used in the experiments, the angle dependence diminishes.

3. Material and methods

3.1. Simulated experiment

The experiment performed by Beck (1992) has been simulated in DEMeter++. This experiment involves a cubic box with edges of 0.707 m oscillating sinusoidally in the vertical direction with an amplitude of 0.03 m at a frequency of 4 Hz. At the bottom of the box, a grating holds back the straw, but allows the grain to pass. Initially the box is filled with straw up to a certain area density. In the next step, the straw is shaken for 20 seconds to randomize it. After the randomization a homogeneous layer of grain is released on top of the shaking straw. A weighing scale underneath the box records the separated grain fraction in function of time. The experiment has been repeated for several grain (0.5, 1 and 2 kg/m^2) and straw area densities (2,3,4,6 and 7 kg/m^2) in order to assess their effect on the penetration time. A significant effect of the straw area density on the separation profiles was found. Only the straw area density of 2 and 3 kg/m^2 could be simulated within a reasonable time frame. Beck (1992) reported that grain area density did not have a significant effect in the tested range so 0.5 kg/m^2 of grain was used in the simulations to reduce computational time.

3.2. Structure of the simulations

Although a real-life separation experiment takes a short time to execute, the corresponding simulation is computationally expensive due to the high number of particles involved. The simulation consists of 5 phases. At some points, the simulation has been changed in comparison to the experiment to shorten the simulation time. First of all, the ground surface of the box has

been reduced by a factor four such that less particles are required to simulate the area densities used in the experiments by Beck (1992). The influence of this intervention has been verified. Additional changes with reference to the experiment will be indicated in the description of the different phases below.

Initialization of the straw layer. The straw is aligned at the bottom of the box in horizontal layers as visualized in Fig. 6. The center lines of the straw particles in a layer are 0.01 m apart, horizontal layers are also at 0.01 m apart. Subsequently, the joints of each straw particle are given a random initial deviation with a maximum of 2.5 mm, because also true straw stems are not completely straight and it reduces the number of contacts at the first moment that the straw particles touch.

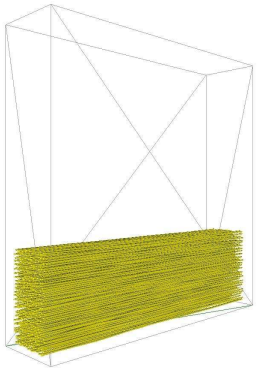

Figure 6: Straw initialization

Randomization of the straw layer. After the initialization of the straw layers the oscillatory motion is started. In this way, the straw is shaken up in the box for 2 s (Fig. 7). As in a real experiment the particles experience aerodynamic drag, this effect has also been implemented in the simulation. The straw randomization was shortened from 20 s in the real experiment to

2 s to reduce the simulation time. The time step of discretization was set to 6 μs. Subsequently, the state of all particles is saved.

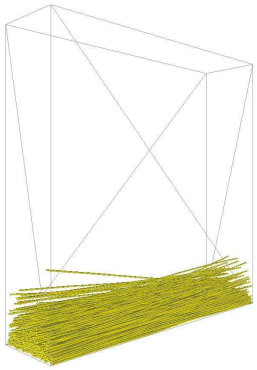

Figure 7: Straw randomization

Grain initialization. The grain particles (0.5 kg/m^2) are randomly spread over the area of the box in one layer at the top of the box (Fig. 8).

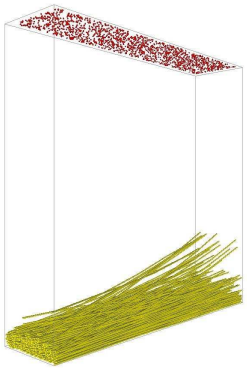

Figure 8: Grain initialization

Grain and straw simulation. After releasing the grain layer above the straw mass, the kernels fall into the box, resisted by aerodynamic drag forces. After about 0.5 s, the kernels reach the top of the straw mass. The straw

restrains the kernels' movement. As the straw is randomized, the particle trajectory lengths as well as their velocity on the trajectories differ. When the kernels approach the grit floor they pass through freely as there is no contact detection between the kernels and the floor of the box (Fig. 9). This differs from physical experiments where a grid floor slightly slows down the grain kernels. This influence is, however, very limited as stated by Beck (1992) because a grid of 1x1 cm^2 with a wire diameter of 1 mm was employed. Due to the large number of contacts between the particles, the time discretization had to be reduced from 6 μs to 2 μs compared to the randomization phase.

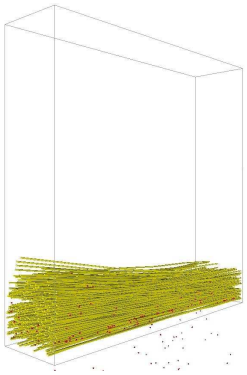

Figure 9: Separation

Post-processing. In the grain simulation step the grain kernels passing through an imaginary plane at 5 cm below the floor of the box are counted. This is different from the experiment described by Beck (1992) where the separated grain fell onto a weighing scale fixed to the base frame of the setup. Consequently, the travelling time of a kernel between the grit floor and the weighing scale depends on the location of the box at the moment of separation, which could introduce small variations between the experimental and simulation

results. For the validation, this does not make any difference because the weighing was done at a much lower frequency than the oscillation of the box. However, from a modeling point of view it is more useful to have the kernels travelling a fixed distance before detection as the distance that the kernel is subjected to aerodynamic drag is constant. Only the plane of detection is moving, for which can be corrected easily.

In post-processing, the cumulative separated fraction is plotted as a function of time.

Summarizing, three simplifications have been introduced in order to make the simulation computationally feasible. First of all, the box size has been reduced, the lowest grain area density employed by Beck (1992) has been employed and the randomization phase has been shortened. These changes allow to simulate the experiment up to 3 kg/m^2 of straw within a reasonable time. Simulating a higher amount of straw particles is currently not feasible because of too long simulation times due to the fact that the DEMeter++ code has not been parallelized yet.

The experimental separation profiles from Beck (1992) start when the first grain kernel is separated. In order to make a valid comparison between the simulated curves and the experimental ones, also the origin of the simulated curves needs to be shifted to the point at which the grain starts to be separated from the straw mass. It was opted for here to use the time at which the fifth grain kernel has left the box as this starting point, as the moment when the first grain kernel is separated was found vary too much.

3.3. Experimental design of the simulations

To validate the DEM modeling of grain-straw separation with bendable straw the simulated separation profiles were compared to the profiles measured by Beck (1992) and the separation profiles resulting from the DEM equivalent. However, Beck (1992) did not report the straw and grain properties of the crop used in his experiments. He only reports that the same crop was used in all experiments. Therefore, DEM simulations have been performed for a range of realistic wheat straw and grain properties. The DEM approach is considered valid when the simulated separation profiles for a set of crop properties at all simulated straw area densities match sufficiently well with the profiles reported by Beck (1992). Beck (1992) performed separation experiments at different grain (0.5 to 2 kg/m^2) and straw densities (2 to 7 kg/m^2). However, he reported that the grain area density had no significant effect on the separation profile. Therefore, simulations have only been performed at a grain area density of 0.5 kg/m^2. Additionally, the simulations were limited to the 2 kg/m^2 and 3 kg/m^2 straw area densities (SAD), because the higher straw area densities could not be simulated for all considered crop properties (see below) within a reasonable time frame.

To limit the required number of simulations, only the crop properties which were expected to have a major influence on the separation profile have been included in the design. For the straw particles these properties are mass per unit length (ML), radius (R) and Young's modulus in bending (E_b). To calculate a realistic mass per unit length of the straw stalk two extra parameters have to be known: density and wall thickness (e). For the grain kernels only the kernel weight (GW) and minor axis radius (GR) are selected. The

minor axis diameter is chosen as the radius of the spherical grain kernels in DEM, ignoring the major axis diameter because the ease of sinking of a particle through a particle bed is mainly determined by the smallest diameter of the particle. Performing DEM simulations for all possible combinations of crop properties (full factorial design) is not computationally feasible due to the number of crop properties and the high computational cost per simulation (on average 21 days computation time). Therefore, a uniform space filling design of crop properties has been constructed in the JMP software (*JMP, The SAS Company, Inc.*, Cary(NC), USA). This design uniformly samples the virtual domain spanned by the crop properties (6) while keeping the amount of necessary simulations as low as possible. To obtain a valid experimental design, the amount of test points needs to be increased with 10 for each dimension added (Fang et al., 2000). Thus, the result is a uniform design with six dimensions: 4 straw properties and 2 grain properties consisting of 60 combinations for which DEM simulations had to be performed. The same experimental design of crop properties has been used for 2 and 3 kg/m^2 straw area density. Using the techniques for crop calibration, the desired crop properties were then translated into simulation parameters. The other crop variables which have to be defined in the DEM simulations were kept constant at the earlier mentioned average values. All 120 simulations have been performed in parallel, each on a 2.8 GHz Intel Xeon 5560 (Nehalem) CPU of the KU Leuven/UHasselt VIC3 High Performance Computing cluster.

3.4. Validation

As the separation profiles have an S shape, 10 candidate sigmoidal equations have been fitted on the separation profiles and judged by their coefficient

of determination and absence of lack-of-fit. The following sigmoidal equation was selected for its accuracy and interpretability (Eq. 7):

$$S(t) = (1 - e^{-a \cdot t})^b \tag{7}$$

Where $S(t)$ is the cumulative separated fraction, a is a measure of the slope of the curve, b shifts the curve to the right. Next, the coefficient of determination between the simulated and the measured profiles has been computed for each of the 60 separation curves of an area density series.

3.5. Sensitivity study

The DEM simulations for the 60 combinations of crop properties of the uniform space filling design at each straw area density provide information on the effect of straw area density and crop properties on the grain separation profiles. The shape of the simulated separation profile associated with each combination of crop properties is described with the a and b parameter of the sigmoidal function fit. Baader et al. (1969), Beck (1992) and Huisman (1978) derived as additional parameter the time to separate a defined fraction of the grain mass, because this gives an intuitive indication of the separation rate. Usually this fraction is taken as 80%, to get the so-called $t_{0.8}$ value. Evaluating Eq. 7 in $t = 0.8$, $t_{0.8}$ can be expressed in function of a and b as:

$$t_{0.8} = \frac{ln(1 - \sqrt[b]{0.8})}{a^2} \tag{8}$$

Next, an all possible subsets regression has been carried out in the JMP software to select the optimal subset of straw area density, crop properties and two-factor interactions for a regression model to predict a, b and $t_{0.8}$.

The subsets that included interaction terms were restricted to exhibit effect heredity so that an active 2-factor interaction will have at least one of its main effects also active. The algorithm outputs the best subset in function of the number of parameters. The optimal number of parameters has been selected based on Akaike's information criterion ($AICc$), the Bayesian Information Criterion (BIC), Mallow's Cp and the adjusted R^2.

4. Results

4.1. Validation of the bendable straw approach for grain-straw separation

The separation profiles associated with the different combinations of crop properties generated with the space filling design are displayed in Fig. 10 for a straw area density of 2 kg/m^2 and in Fig. 11 for 3 kg/m^2. These 60 different separation curves show that the influence of crop properties on separation is substantial, as a large variation is present. Also a 4 Hz modulation due to the oscillation of the box, is visible on the separation curves. It can be observed that a number of simulated curves correspond well to the experimental ones.

The coefficient of determination (R^2) between the simulated and the experimental data is computed for each of the 60 separation curves of an area density series. As shown in Table 2, eight different combinations of crop properties deliver an R^2 value over 0.98 for both straw densities. It is remarkable that several, apparently unrelated combinations of crop properties are able to match the experimental separation profiles of Beck (1992). This indicates again the complex interactions of the crop properties underlying separation.

Table 2: Crop properties of good fitting DEM simulations of 2 and 3kg/m^2

	Straw properties			**Grain properties**			
	R	ML	E_b	GR	GW	R^2_{2kg/m^2}	R^2_{3kg/m^2}
	$(10^{-3}m)$	$(10^{-3}kg/m)$	(GPa)	$(10^{-3}m)$	$(10^{-5}kg)$		
Range	[1.42,1.73]	[0.85,1.54]	[1.28,6.00]	[2.54,3.50]	[3.30,5.08]		
1	1.69	1.48	3.81	2.93	4.33	0.99	0.98
2	1.59	1.39	3.04	3.16	4.50	0.99	0.99
3	1.65	1.25	2.64	2.62	4.65	0.99	0.99
4	1.63	1.32	4.23	2.73	5.03	0.99	0.99
5	1.61	1.26	3.13	2.69	3.84	0.99	0.99
6	1.63	1.46	2.97	3.22	3.39	0.99	0.99
7	1.69	1.45	5.58	2.74	3.61	0.99	0.99
8	1.60	1.23	1.42	3.06	3.56	0.98	0.99

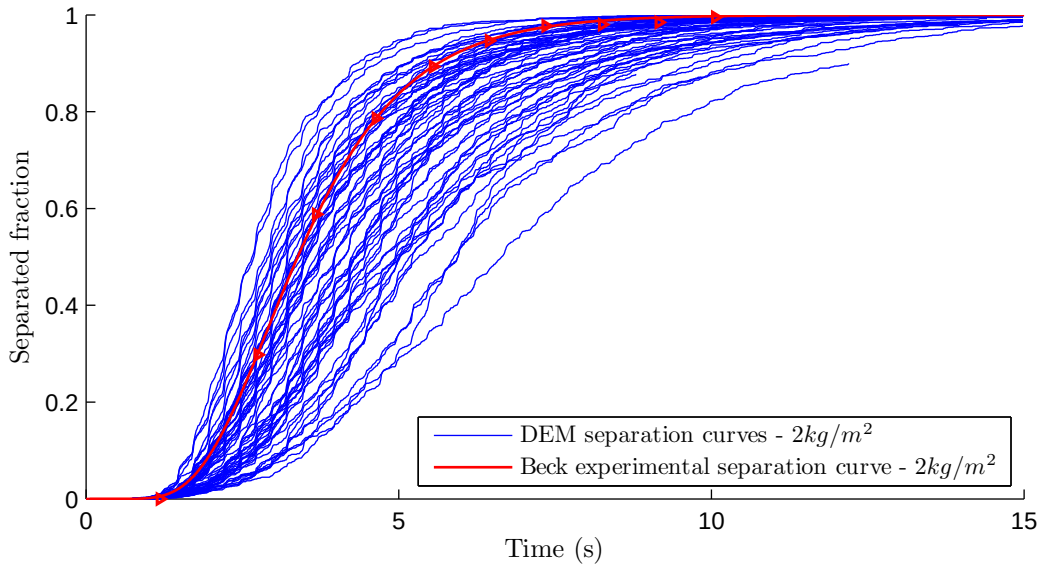

Figure 10: Separation curves resulting from the uniform space filling design for a straw area density of 2 kg/m^2

It can be observed that the simulations matched generally better with the higher straw radii (R) and the higher straw masses of the experimental design. However, a simulation with a high straw mass and high grain diameter can for instance result in a similar separation profile to a simulation with a low straw mass and a small grain diameter. This suggests that certain crop properties have similar or opposite effects on separation. Beck (1992) used one type of crop for the experiments. Also here, the same sets of crop properties provide successful matches at both straw area densities.

It can be concluded from the high coefficients of determination and the fact that similar optimal combinations show up in both area densities that the experimental separation profiles from Beck (1992) can be reproduced with

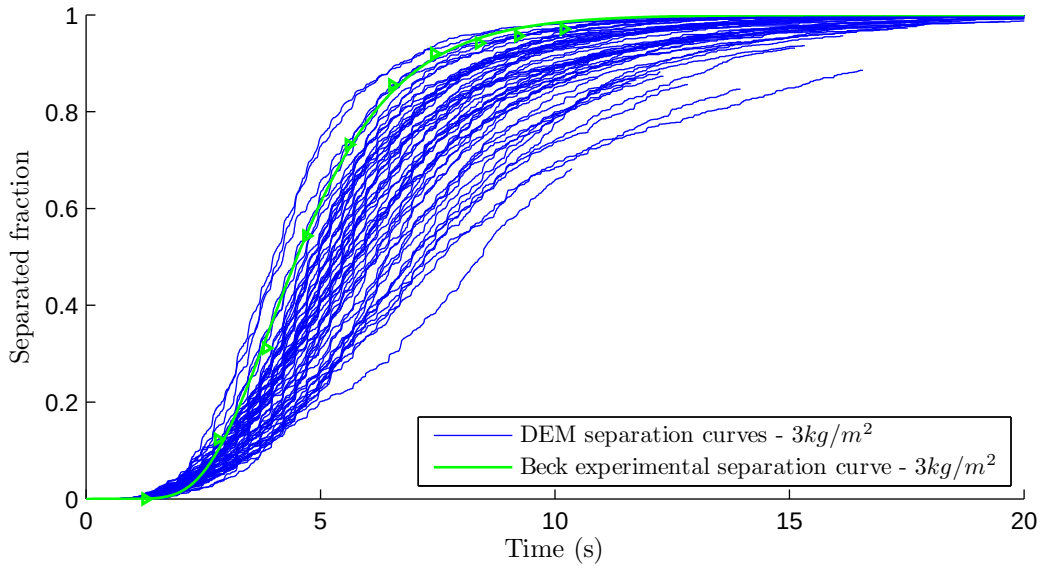

Figure 11: Separation curves resulting from the uniform space filling design for a straw area density of 3 kg/m^2

a DEM simulation using bendable straw particles and grain with realistic properties. This endorses DEM as a tool to perform grain-straw separation experiments. However, it is not possible to point out one single best set of crop properties. This is due to two facts: First, there is a large variation on the position of each separation curve due to the randomness in grain kernel initialization. Secondly, some crop properties have similar or opposite effects on separation, which makes different combinations of realistic crop properties feasible. In order to get a better insight in the influence of individual crop properties on separation, a sensitivity analysis has been conducted and the results are presented in the next section.

4.2. Sensitivity study of particle properties on grain-straw separation

An all possible subsets regression has been performed to find the combination of straw area density (SAD) and crop properties that gives the best prediction of the a, b and $t_{0.8}$ parameters of the sigmoidal fit to the simulated separation profiles. The coefficients of the regression functions for a, b and $t_{0.8}$ are shown in Table 3. The selected models for a and $t_{0.8}$ have a high coefficient of determination (both $R^2 = 0.80$), while the one for b does not ($R^2 = 0.44$). All effects included in the table are significant ($P < 0.05$). As can be seen, all main effects are active ($P < 0.05$), except grain kernel weight for $t_{0.8}$. A limited number of interaction terms is active ($P < 0.05$), but not consistently.

In the range of a ($[0.3, 1]$) and b ($[5, 20]$), the gradient of t_08, derived from Eq. 8 in the direction of a varies between -50 and -3 while in the direction of b it varies from 0.05 to 0.65. This means that the effect of b on the separation rate is small, compared to the effect of a.

The main effects on a have the same sign of the effects on $t_{0.8}$, which is not the case for the main effects on b. Due to the predominance of the effect of a on separation rate and the low correlation with b, the sensitivity study will be confined to the effect of crop properties on a and $t_{0.8}$. Looking at the observations by Beck (1992), however, it is likely that the effect if b will become more pronounced at straw area densities higher than the ones simulated in this research. When comparing Fig. 10 to 11, slower separation is noticed at higher straw area density. The increased path length of the grain, with higher probability of dispersion after collision with the straw particles, results in slower separation. This is confirmed by the observations

of all previously cited separation studies. The slower separation translates in a higher b value while the increased dispersion flattens the separation profile, resulting in a lower a value. Both effects combine into a higher separation time $t_{0.8}$. Also the effects of the straw radius R and the mass per unit length of the straw particles ML have to be viewed in that light. A higher straw radius will result in higher straw coverage and likewise in a higher probability of collision of the grain with straw particles. This results in a lower a value, a higher b value and a higher $t_{0.8}$. As the simulations have been carried out with a fixed straw area density, a higher mass per unit length (ML) means that the total amount of straw stalks will be lower, thus reducing the thickness of the straw layer and speeding up separation. However, if the stalks become heavier, they will be thrown less high by the oscillating box, implying that the straw mass stays more dense and by this is harder to penetrate, but apparently the reduction in the amount of straw particles is more dominant. A higher bending stiffness of the straw (E) decreases the separation speed. It was observed that less bendable straw particles stay more aligned in the box. In this way they pack densely and restrain the kernels more. This effect is even amplified at higher straw area densities and higher straw radii, as indicated by the active interaction of E and SAD. Increasing grain radius (GR) slows down separation. This confirms the observations of Gregory and Fedler (1986) and Shandilya (1987). This can possibly be explained by the fact that small grain kernels can penetrate much narrower voids. The negative sign for the interaction between GR and R indicates that the effect of grain radius decreases when increasing the straw radius which suggests that separation speed depends on the relative size of the particles involved,

which is rather intuitive.

4.3. Computational requirements

All simulations have been executed in parallel on a separate processor core. The average computing time depended on the number of particles involved in the simulation. On average, it took 10 h to compute a second of simulation for a straw area density of 2 kg/m^2 and 24 h for a straw area density of $3kg/m^2$, both with the reduced box size. For $2kg/m^2$ also shortened simulations with the full box were done. this took 139 h per second of simulation, making validations with the full box size computationally infeasible. For $3kg/m^2$ no comparison was made. Even though the computations have been executed on modern CPU's, computational power stands in the way of a full validation. DEM simulations can be accelerated by running the simulations on a graphics processing unit (GPU) instead of a central processing unit (CPU) or by parallellization of DEMeter++ allowing the use of multiple cores for one simulation. The new upcoming version of DEMeter++ promises a 20-fold increase of the calculation speed. If applied in parallel, an additional gain of a factor 6 is expected.

5. Conclusions

In this research, grain-straw separation was simulated with spherical grain particles and segmented straw particles made up of cylindrical and spherical DEM primitives. Before conclusions were drawn concerning the influence factors on grain-straw separation, the approach was successfully validated against the experiments of Beck (1992). A number of candidate sets of crop properties have been found to fit both the 2 and 3 kg/m^2 straw area densities

Table 3: Coefficients of the crop simulation parameters in all possible subsets regression

	a ($R^2 = 0.80$)	b ($R^2 = 0.44$)	t_{08} ($R^2 = 0.80$)
Intercept	1.69	1.50	-6.35
SAD	-1.80 10^{-1}	6.20 10^{-1}	2.34
R	-4.29 10^{2}	6.96 10^{2}	4.47 10^{3}
ML	5.99 10^{2}	1.09 10^{2}	-6.58 10^{3}
E_b	-1.55 10^{-2}	1.50 10^{-1}	1.31 10^{-1}
GR	-2.14 10^{2}	-1.44 10^{2}	2.18 10^{3}
GW	-7.53 10^{2}	-1.59 10^{4}	
$SAD_n \cdot E_{b,n}$	4.92 10^{-2}		3.50 10^{-1}
$SAD_n \cdot R_n$		-7.32 10^{3}	
$SAD_n \cdot ML_n$		6.53 10^{3}	
$SAD_n \cdot GR_n$		-1.69 10^{3}	
$R_n \cdot E_{b,n}$	4.03 10^{2}	2.08 10^{3}	1.45 10^{3}
$R_n \cdot GR_n$	-8.05 10^{5}		
$R_n \cdot GW_n$	-5.00 10^{7}	-4.75 10^{8}	
$ML_n \cdot E_{b,n}$	-1.64 10^{2}	-9.02 10^{2}	

Legend: $SAD_n = SAD - 2.50$; $R_n = R - 1.5710^{-3}$; $ML_n = ML - 1.1710^{-3}$; $E_{b,n} = E - 3.64$; $GR_n = GR - 3.0210^{-3}$; $GW_n = GW - 4.2210^{-5}$;

experiments well. Therefore, it was concluded that different combinations of crop properties lead to the same separation rate. To find out in which direction and to which extent the properties influence separation, also a sensitivity study was done on the available runs. Different correlations for the different straw area densities were found. All crop properties were found to influence the separation speed, but the main influences can be related to straw coverage and grain kernel diameter. The fastest separation occurs in straw with thin but stiff (in bending) and heavy stalks. This can be the result of a thick straw wall in combination with a high wall density. These heavy stalks result in a low number of stalks needed for a certain straw area density and their small radius gives a low coverage. A low stiffness in bending gives a high porosity of the straw mat that is easy to penetrate by the grain kernels. The smaller the radius of these kernels, the more free paths are available, which results in a faster separation. The effect of moisture on separation, observed in several researches, affects the particle interactions leading to separation indirectly, by its influence on the mechanical particle properties such as the bending stiffness. The relation between these properties and moisture can be found in for instance Sitkei (1986) and Mohsenin et al. (1986).

The DEM-particles developed in this work can be easily applied in combination with more complex geometries such as the walker section of a conventional combine harvester. As Beck (1992) used unthreshed straw stalks of which the ears were cut, also the properties of unthreshed stalks have been used in this publication. To simulate a walker section, however, the mechanical properties of threshed, and thus possibly damaged, straw should be measured and employed. Besides, also break-up of stalks can occur. Therefore,

the size distribution of the particles fed to the walkers, which was considered as an important factor for separation speed by Huisman (1978) should correspond to the one in the real combine. To simulate additional straw break-up on the walkers, also breakable bonds between the straw segments should be implemented in the DEMeter++ software.

6. Acknowledgements

Bart Lenaerts is funded by the Institute for the Promotion of Innovation by Science and Technology in Flanders (IWT-Vlaanderen) through Baekeland project 090720 in collaboration with Case-New Holland Belgium n.v.. Engelbert Tijskens and Bart De Ketelaere are funded by the Industrial Research Fund (IOF). The authors gratefully acknowledge the Hercules foundation and the Flemish Government -department EWI for funding the VSC - Flemish Supercomputer Center at which the simulations have been performed.

7. References

Annoussamy, M., Richard, G., Recous, S., Guerif, J. et al. (2000), 'Change in mechanical properties of wheat straw due to decomposition and moisture.', *Applied Engineering in Agriculture* **16**(6), 657–664.

Baader, W., Sonnenberg, H. and Peters, H. (1969), 'Die entmischung eines korngut-fasergut-haufwerkes auf einer vertikal schwingenden, horizontalen unterlage', *Grundlagen der Landtechnik* **19**(5), 149–157.

612 Beck, T. (1992), Meßverfahren zur Beurteilung des Stoffeigenschaftseinflusses
613 auf die Leistung der Trennprozesse im Mähdrescher. Fortschritt-Berichte
614 VDI Reihe 14 Nr. 54, PhD thesis, Dissertation Universität Stuttgart.

615 Cundall, P. and Strack, O. (1979), 'A discrete numerical model for granular
616 assemblies', *Geotechnique* **29**(1), 47–65.

617 Fang, K.-T., Lin, D. K., Winker, P. and Zhang, Y. (2000), 'Uniform design:
618 Theory and application', *Technometrics* **42**(3), 237–248.

619 González-Montellano, C., Ayuga, F. and Ooi, J. (2011), 'Discrete element
620 modelling of grain flow in a planar silo: influence of simulation parameters',
621 *Granular Matter* **13**(2), 149–158.

622 Gregory, J. and Fedler, C. (1986), 'Mathematical relationship predicting
623 grain separation in combines', *American Society of Agricultural Engineers.*
624 *Microfiche collection* .

625 Haff, P. and Werner, B. (1986), 'Computer simulation of the mechanical
626 sorting of grains', *Powder Technology* **48**(3), 239–245.

627 Hall, J. and Husman, J. (1981), Correlating physical properties with combine
628 performance, *in* 'Proceedings of the 1981 ASAE Winter Meeting, Decem-
629 ber', pp. 15–18.

630 Huisman, W. (1978), 'Moisture content, coefficient of friction and modulus
631 of elasticity of straw in relation to walker losses in a combine harvester'.

632 Iwai, T., Hong, C. and Greil, P. (1999), 'Fast particle pair detection algo-

rithm for particle simulations', *International Journal of Modern Physics C* **10**(5), 823–837.

Kattenstroth, R., Harms, H.-H. and Lang, T. (2011), Systematic alignment of straw to optimise the cutting porcess in a combine's straw chopper, *in* 'Proceedings of Land.Technik AgEng 2011,November 11-12 2011, Hannover (Germany)'.

Kutzbach, H. (2003), Approaches for mathematical modelling of grain separation, *in* 'Electronic-only proceeding of the international conference on crop harvesting and processing. Kentucky, USA'.

Landry, H., Laguë, C. and Roberge, M. (2006), 'Discrete element modeling of machine–manure interactions', *Computers and electronics in agriculture* **52**(1), 90–106.

Mohsenin, N. N. et al. (1986), 'Physical properties of plant and animial materials (revised). structure, physical characterisitics and mechanical properties.', *Physical properties of plant and animial materials (Revised). Structure, physical characterisitics and mechanical properties.* .

O'Dogherty, M., Huber, J., Dyson, J. and Marshall, C. (1995), 'A study of the physical and mechanical properties of wheat straw', *Journal of Agricultural Engineering Research* **62**(2), 133–142.

Shandilya, A. (1987), Effect of grain type and straw type on separation in combines, Master's thesis, Texas Tech University.

Sitkei, G. (1986), *Mechanics of agricultural materials*, Elsevier Science Pub. Co. Inc., New York.

656 Srivastava, A., Mahoney, W., West, N. et al. (1990), 'The effect of crop
657 properties on combine performance.', *Transactions of the ASAE* **33**(1), 63–
658 72.

659 Stroshine, R. (2000), 'Physical properties of agricultural materials and prod-
660 ucts', *Department of Agricultural and Biological Engineering, Purdue Uni-*
661 *versity, West Lafayette, Indiana* .

662 Tavakoli, H., Mohtasebi, S. and Jafari, A. (2008), 'A comparison of mechani-
663 cal properties of wheat and barley straw', *The CIGR Ejournal Manuscript*
664 *number CE 12 002* **10**.

665 Tijskens, E., Ramon, H. and Baerdemaeker, J. (2003), 'Discrete element
666 modelling for process simulation in agriculture', *Journal of sound and vi-*
667 *bration* **266**(3), 493–514.

668 Van Liedekerke, P., Tijskens, E., Dintwa, E., Rioual, F., Vangeyte, J. and
669 Ramon, H. (2009), 'Dem simulations of the particle flow on a centrifugal
670 fertilizer spreader', *Powder Technology* **190**(3), 348–360.

671 Wright, C., Pryfogle, P., Stevens, N., Steffler, E., Hess, J. and Ulrich, T.
672 (2005), Biomechanics of wheat/barley straw and corn stover, *in* 'Twenty-
673 Sixth Symposium on Biotechnology for Fuels and Chemicals', Springer,
674 pp. 5–19.

Appendix A. List of abbreviations

a	model parameter
a_i	acceleration (m/s^2)
A	particle area (m^2)
$AICc$	Akaike's information criterion
b	model parameter
BIC	Bayesian infromation criterion
C_p	Mallow's criterion
dl	Bending deformation (m)
e	straw wall thickness (m)
E_b	Young's modulus in bending (GPa)
E_e	Young's modulus in tension (N/m^2)
F_b	straw bending force (N)
F_c	contact force (N)
F_e	extension force (N)
G, H	body forces (N)
GR	grain radius (m)
GW	grain weight (kg)
I	inertia tensor $(kg \cdot m^2)$
I_b	second moment of area (m^4)
k	spring constant (N/m)
L	straw length (m)
m	mass (kg)
ML	straw unit mass (g/m)
R	straw radius (m)
r_c	position of contact w.r.t. center of mass of particle (m)
S	cumulative separated fraction
t	time (s)
α_i	rotational acceleration (rad/s_2)
Δt	time step (s)
$t_{0.8}$	time to separate 80% of the grain mass (s)